COMPUTED ATMOSPHERIC EFFECTS ON ERTS OBSERVATIONS

Robert S. Fraser, *Goddard Space Flight Center, Greenbelt, Maryland 20771*

ABSTRACT

The nadir radiances of many models of the earth-atmosphere system were computed for a fixed solar zenith angle. These data indicate that the standard deviations of the Multispectral Scanner responses to changes in water vapor and aerosols would be small on a continental-wide basis.

The computed effects of the atmosphere on ERTS observations are usually not large. Data given at this symposium in other papers show that the path radiance of just the atmosphere can be strong and quite variable, which is true. However, that is not the whole story. The radiant energy that arrives at a satellite can be separated into two parts: the path radiance just mentioned and also the light transmitted from the ground directly through the atmosphere without interacting with it. The remarkable thing is that the two parts tend to change in opposite directions, thereby tending to compensate each other. For example, if the atmospheric-turbidity increases, the path radiance increases but the atmospheric transmission decreases. Mother Nature is trying to help the Principle Investigators.

The light scattered by the atmosphere to ERTS-1 depends on the following variables: the solar zenith angle, the surface reflectivity, the presence of clouds even when there is a clear line-of-sight between the satellite and a surface target, water vapor, and particulates. The atmospheric models used for the computations that are presented here are free of clouds. The point that will be developed in this report is that for a fixed solar zenith angle the atmosphere would appear to cause only small variations over a large region such as the continental United States. The atmsophere can cause significant effects near strong pollution sources such as big cities; but on a continental basis the computed atmospheric effects are small.

Particulates play an important role in atmsopheric scattering. Although their sizes range over three orders of magnitude, only those particulates with radii between 0.1 and 1 μm have a significant effect on the ERTS observations. Figure 1 shows this fact for a small volume of slightly absorbing particulates. The size distribution function is

inversely proportional to the particle radius to the fourth power.
Such a law applies for average conditions near the surface of conti--
nental regions (Junge, 1963). One-half of the mass of such particulates
consists of those with radii less than one micrometer and the particles
with the remaining mass have radii between one and 10 micrometers, as
shown in Fig. 1. However, the cumulative extinction curve shows that
the particles smaller than one micrometer account for 90 percent of the
attenuation in a beam of light. The inset curve for the probability
density function shows that the particles with 0.2 μm radius have the
strongest interaction with light of wavelength 0.55 μm. Computations
of the extinction characteristics of many models of atmospheric aerosols
show that particles with diameter about equal to the wavelength inter-
act more strongly with the light than other particles.

The particles that scatter sunlight most effectively towards the
zenith are still smaller. If the solar zenith angle is 30° - 40°, the
scattering angle towards the zenith is 150° - 140°. Figure 2 gives the
probability density functions for light scattered in these directions.
They are strongly peaked at a radius of 0.1 μm. Particles larger than
1 μm radius scatter essentially no light towards the zenith.

Models of the atmosphere used for computations given here are free
of clouds, contain the invariant gases, 316 Dobson units of ozone, water
vapor, and particulates. The mass loading of the particulates varies
from none to the mean value plus two standard deviations, except in
Fig. 4. The corresponding turbidity factor, which is the ratio of the
total vertical optical thickness to the optical thickness of just the
scattering gases, is at λ = 0.55 μm 1.3 for no particulates, 3.3 for an
average continental amount, and 5.3 for two standard deviations above
the mean. Shifrin and Shubova (1964) have measured the standard devi-
ation of the turbidity factor and found it to be one-half. However, a
much larger standard deviation of two is computed from values of sur-
face extinction that were measured by Koprova (1971). Most surface
extinction coefficients support the smaller value of one-half though.
A standard deviation of the turbidity factor of one is assumed here.
The indices of refraction of the particulates are either 1.5 or 1.5 -
0.03 i. They are assumed to be spheres, which is known to be an
approximation when the particles are solid.

Water vapor absorption does not affect the first three bands of
the ERTS Multispectral Scanner, but has a strong effect on the 0.8 -
1.1 μm band. The total amount of precipitable water in a vertical
column varies from 1.5 cm to 4.4 cm, which applies in a warm, moist
tropical atmosphere. The surface of the earth is assumed to be homo-
geneous and reflect light isotropically according to Lambert's law.

The numerical computations utilizing the models have an internal
consistency of three significant figures. The computed nadir radiances
for a model atmosphere with a mean turbidity factor of 3.3 at

λ = 0.55 µm are compared with measured values in Fig. 3. The observat
tions were made from aircraft east of Cape Hatteras in a cloud-free
region. The values of the surface reflectivity used in the calcula-
tions were those derived from measurements made at a height of 0.3 km.
The measured and computed values agree fairly well. The model can be
adjusted to decrease the discrepancies, but the exercise is not fruit-
ful since the true aerosol state at the time of the measurements is not
known.

The net effect of both the atmospheric transmission and path
radiance on the ERTS observations is important.and not just either one
alone. Either factor can be large, as shown for the path radiance in
Fig. 4, which gives the relative contribution of path radiance to the
total radiance. The turbidity factors are 1.3, 4.3, and 13.3 for
successive curves from the lowest to the highest. The middle curve
represents more or less average turbidity. The path radiance decreases
from 100 percent when the ground is black to a significant fraction of
37 percent when the surface reflectivity is 1.0. Also, the fraction of
airlight increases significantly as the turbidity increases.

However, Fig. 5 shows that when the trade-off between path
radiance and transmission are accounted for, the net change is sensor
response for an atmosphere without particulates to one with average
loading is less than 10 percent if the surface reflectivity is greater
than 0.1. The effect of particulates is greatest over dark surfaces
such as water. The effect for all the MSS channels is similar to those
given by the two curves.

An estimate of the two standard deviations ranges of the ERTS MSS
sensor responses are given in Fig. 6. These data are based on the
computations for the many models already discussed; but the ranges are
based on educated guesses concerning the atmospheric aerosols, since
the statistical characteristics of the aerosol state are not known.
The mean sensor response for each spectral band is nearly a linear
function of the surface reflectivity, as has been noted before. The
sensor response for the 0.8 - 1.1 µm is lower than those of the other
bands because the sensor gain is lowest for the 0.8 - 1.1 µm band and
significant water vapor absorption occurs in this band but not in the
others. The ratio of the standard deviation, which is one-fourth the
height of the bars on the graph, to the mean is small. For example,
when the surface reflectivity is 0.2, the ratio is about 5%. This
variability can be compared with the ultimate achievable accuracy in
making atmospheric corrections, which is related to the National
Bureau of Standards' Calibration Lamps. They have an accuracy of only
5 percent. The atmospheric variability should be measured by many
high altitude observations of different surfaces whose reflectivities
are constant. Such data are expensive to acquire by aircraft. The
ERTS-1 MSS measurements may be satisfactory for this purpose.

The ratio of the standard deviation of the nadir radiances, which are derived from the data on Fig. 6, to the noise equivalent radiances (NER) of the MSS sensor systems are given in Fig. 7. The NER's were measured before ERTS-1 launch. The variation is appreciable in the 0.5 - 0.6 µm channel, but in the remaining bands the variations are comparable to the NER's. If the radiance variation caused by the atmosphere is comparable to the NER's of future ERTS' sensors, then no attempt need be made to correct for the atmosphere.

Future studies of atmospheric effects should be directed towards solving well-defined problems. The atmosphere does not seem to have an important effect on current ERTS-1 observations, except for water observations. The data given here indicate that the effects will be weak when considering a large region and large length of time. Operational methods to correct for atmospheric effects appear to be expensive. Such corrections would also add to the heavy burden of data reduction systems. Therefore, development of an operational system to correct for atmospheric effects should be based on need and then on the capability of making the corrections.

REFERENCES

1. Junge, C. E., "Air Chemistry and Radioactivity," Academic Press, New York.

2. Koprova, L. I., Izv., Atms. Oceanic Phys. $\underline{7}$, 415 (1971).

3. Shifrin, K. S. and Shubova, G. L., Izv., Geophys. Ser., 161 (1964).

FIGURE CAPTIONS

Fig. 1. The probability density of extinction (inset), the cumulative probability of extinction, and the cumulative probability of mass of atmospheric particulates as functions of their radius. The size distribution function of the number of particulates is inversely proportional to the fourth power of the radius. The index of refraction of the particulates is 1.5 - 0.03 i. The wavelength is 0.55 μm.

Fig. 2. The probability densities of the light scattered in the directions 140° or 150° as functions of radius. The parameters are given in the Fig. 1 caption.

Fig. 3. Comparison of measured and computed spectral radiances of the nadir over the ocean. Measurements were made by Hovis in July 1972.

Fig. 4. The computed ratio of the path radiance to the total radiance of the earth-atmosphere system in the nadir direction. The index of refraction of the particulates is 1.5. The solar zenith angle is 40°. The wavelength is 0.55 μm.

Fig. 5. The relative increse in the MSS sensor response to the nadir radiance when the atmospheric model without particulates adds the average amount of particulates. The size distribution function of the particulates is inversely proportional to the fourth power of the radius. The index of refraction of the particulates is 1.5. The solar zenith angle is 40°.

Fig. 6. Range of sensor responses in the 4 MSS spectral bands to the nadir radiance. The estimated variation is plus and minus two standard deviations. The number above each set bands is the surface reflectivity. The solar zenith angle is 40°.

Fig. 7. The ratio of the standard deviation of nadir radiances, which are derived from Fig. 6, to the noise equivalent radiances of the MSS sensors.
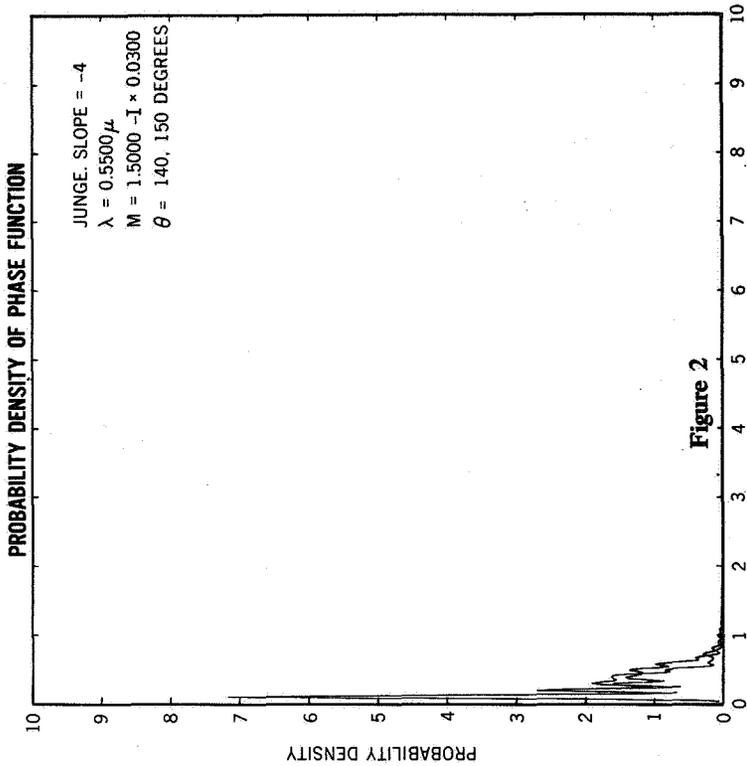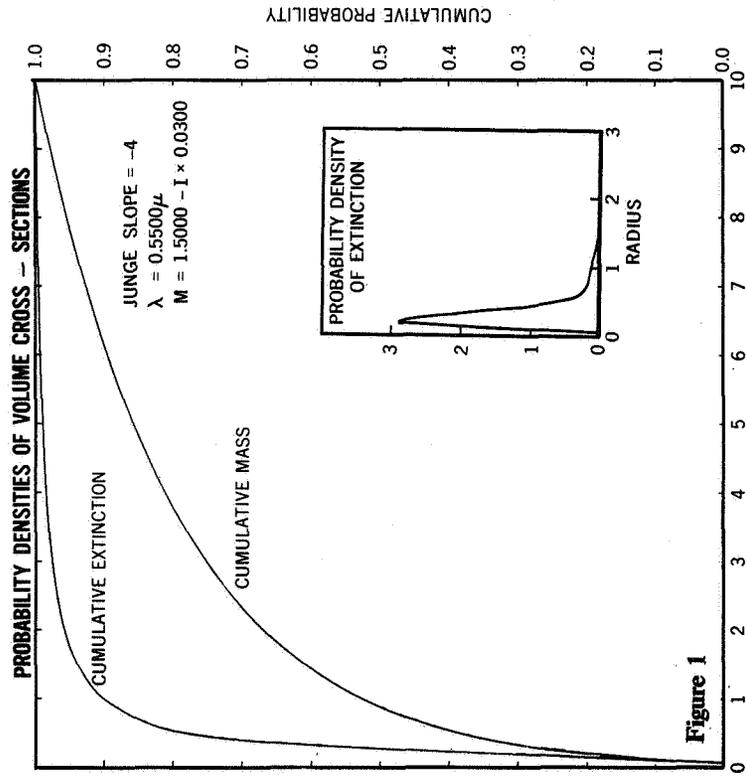
1571

Figure 1

PROBABILITY DENSITIES OF VOLUME CROSS − SECTIONS

JUNGE SLOPE = -4
$\lambda = 0.5500\mu$
$M = 1.5000 - I \times 0.0300$

CUMULATIVE EXTINCTION

CUMULATIVE MASS

RADIUS IN MICRONS

CUMULATIVE PROBABILITY

PROBABILITY DENSITY OF EXTINCTION

RADIUS

Figure 2

PROBABILITY DENSITY OF PHASE FUNCTION

JUNGE. SLOPE = -4
$\lambda = 0.5500\mu$
$M = 1.5000 - I \times 0.0300$
$\theta = 140, 150$ DEGREES

RADIUS IN MICRONS

PROBABILITY DENSITY

Figure 3

NADIR RADIANCE IN MW/ (CM²−MICROMETER−STERAD)

MEASURED AT 11.4km

COMPUTED

MEASURED AT 0.3km

WAVELENGTH (MICROMETERS)

Figure 4

0.5 − 0.6 μm BAND MSS

TURBIDITY FACTOR   VSBY

13.3   3.3 km

4.3   13.0

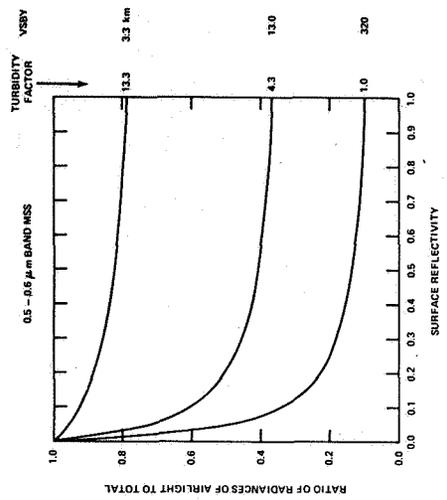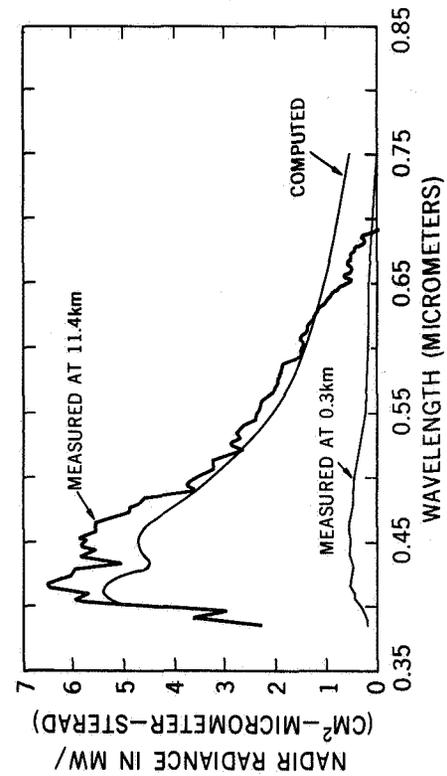1.0   320

SURFACE REFLECTIVITY

RATIO OF RADIANCES OF AIRLIGHT TO TOTAL

RELATIVE CHANGE IN NADIR RADIANCE CAUSED BY PARTICULATES

Figure 5

$\nu^* = 3$
$m = 1.5$

- - - $\lambda 0.55\ \mu m$
—— $\lambda 0.75\ \mu m$

y-axis: $\dfrac{V_{3.3}-V_{1.3}}{V_{3.3}} * 100$

x-axis: SURFACE REFLECTIVITY

Figure 7

0.5 – 0.6 μm

0.8 – 1.1 μm

y-axis: σ_N/NER

x-axis: SURFACE REFLECTIVITY

y-axis: SENSOR RESPONSE IN PERCENT OF FULL SCALE

x-axis: MSS CHANNEL NUMBER

0.00 0.02 0.10 0.20 0.50

Figure 6